

FINITE ELEMENT MODEL OF THE HUMAN LOWER EXTREMITY SKELETON SYSTEM IN A LATERAL IMPACT

*J.K. Yang, A. Wittek, and J. Kajzer
Dept of Injury Prevention, Chalmers University of Technology
Gothenburg, Sweden*

ABSTRACT

This paper presents a finite element model of the human lower extremity skeleton system to facilitate the investigation of dynamic responses of the lower extremity to lateral impact loading. The model consists of the femur, the tibia, and the knee ligaments. The geometry and mass distribution of the model were chosen to represent a 50th percentile male lower extremity skeletal structure based on anatomical measurements and available data. The model was constructed using solid hexahedron elements, shell elements and nonlinear spring-damper elements. Linear viscoelastic material was used to describe the mechanical property of the long bones. Boundary conditions were defined in accordance with the configuration of a car-pedestrian lateral collision.

The model was implemented by means of the finite element program DYNA3D. The tibia segment of the model was validated against the published three-point bending test with human leg specimens. The whole model was validated against previously performed tests with lower extremity specimens at impact speeds of 30 and 17 km/h. A stress analysis was performed in terms of the injury mechanism of the lower extremity to a lateral impact loading. The calculated peak tensile stress in the model at impact speed 30 km/h is 160 MPa which corresponds to the stress level of failure of the tibia. At impact speed 17 km/h the peak tensile stress is 102 MPa that is lower than the ultimate tensile stress of the tibia.

The model facilitates the calculation of detailed physical quantities such as stress distribution within simulated structures, and contributes to a better understanding of injury mechanisms at the level of stress analysis.

THE INJURY MECHANISMS of the human lower extremity in car-pedestrian collisions have been widely investigated in experimental studies with human cadaver specimens (Kramer, et al., 1973; Pritz, 1978; Bunketorp, 1983; Aldman et al., 1985). In these studies, fracture of the tibia or/and failure of the knee structure were frequently observed. However, injury mechanisms and tolerance levels of these body segments were only investigated in terms of measurements of dynamic responses, and dissection and damage inspection of the specimens after impact tests. Important parameters, such as stress/strain distribution within the biological structure cannot be assessed in laboratory tests with biological specimens. Therefore, numerical evaluations of the dynamic response of the human body segments in car-pedestrian collisions supplement experimental studies.

Generally speaking, two approaches are commonly used in the mathematical modeling of human body segments: (1) modeling with the multibody system (MBS); (2) modeling with the finite element method (FEM). A MBS model of the lower extremity with a human-like knee joint has been developed to investigate the dynamic response and predict the injury risk of the knee and the leg to a lateral impact loading (Yang and Kajzer, 1992; Yang et al., 1995). Ishikawa et al. (1993) developed a MBS model of a pedestrian and analyzed the influence of car-front components to impact response of the pedestrian model. The MBS

models are useful to predict kinematics, forces, accelerations etc. in a dynamic system. However, these models cannot be used to calculate the detailed quantities within the human tissues such as stress and strain distribution. This disadvantage can be solved by using the finite element method.

Three main problems should be taken into account in finite element modeling of the lower extremity: (1) the application of an appropriate type of finite elements for the structural modeling, (2) the appropriate material models and material properties of bones and soft tissues, and (3) the complex geometry of the lower extremity skeleton system. So far, in many models, attention has been focused on the geometry of the external surface of long bones.

Defining complex geometry is a difficult and time-consuming task, especially when the solid hexahedron element is used to construct a long bone model. For this reason most long bone models with a refined geometry are described using shell elements (Bermond et al., 1993; Bedewi, 1996). However, using a shell model is not sufficient for investigating the stress distributions within long bones. Furthermore, bones are unhomogeneous material exhibiting viscoelastic properties. In previous studies (Hobatho et al., 1991; Bermond et al., 1993), the long bones have been usually assumed to be homogeneous, isotropic, linear and elastic. However, ignoring viscoelastic properties of long bones may significantly affect the response of the model to transient loads.

The present study was aimed at developing a three dimensional FEM model of the lower extremity skeleton system to explore stress/strain fields in the long bones and knee when the leg is subjected to lateral impact loading. In order to obtain a more accurate stress distribution in the long bone models, the tibia and femur were simulated with solid elements. The mechanical properties were defined as unhomogeneous in long bone models and described using the viscoelastic material law. The correlation between the calculated data and failure of the long bones to a lateral impact loading was investigated. This study shows that the FEM model of the lower extremity skeleton system can be used to predict the risk of injury to the long bones and the knee associated with car-pedestrian collision accidents.

METHOD AND MATERIAL

The finite element program DYNA3D (Hallquist, 1991) was used for modeling the lower extremity skeleton system. Attention was focused on the material and structural modeling of the femur, the tibia and the knee joint complex, which mainly sustain dynamic loading in a lateral impact. The geometry and structure of the lower extremity skeleton system was simplified due to the complexity of the problem and the necessity to define smooth meshing in the impacted area and in articular contact surfaces. Therefore, the patella, the fibula and the meniscus were not introduced into the model.

CONFIGURATION OF THE MODEL - Based on anatomical measurements (Kajzer, 1991) and available anatomical data from the literature (Nyquist et al., 1985), the dimensions and mass distribution of the long bones were defined to represent the lower extremity of a 50th percentile male. The mesh layout of the lower extremity skeleton model was generated by using the pre-processor INGRID. The whole lower extremity skeletal model was supported by a plane which represented the ground. The friction coefficient between foot and ground was assumed to be 0.5.

The Femur - The femur is the longest bone in the body with an approximately cylindrical shape along its shaft and with an upper rounded head. The lower end of the femur consists of the condyles with articular surfaces that match the tibial plateau to form the knee joint. Due to its structure and material properties, the femur the strongest bone in the body is stiff. The femur model was represented by 3072 eight-node solid hexahedron elements. The shaft of the femur model was constructed as a cylindrical shape and was symmetrical about the longitudinal axis. The distal end of the femur model was enlarged to form the femur condyles with their curved surfaces. The rounded head in the proximal end was not described in the present study.

The Tibia - The tibia is the second longest bone in the body. The proximal part of the tibia is enlarged to form the tibia condyles and a flattened area, the tibia plateau. The tibia model was represented by 5364 eight-node solid hexahedron elements. The shaft of the tibia

model was constructed with a cylindrical surface outside and ellipsoidal surface inside, and was symmetric about the longitudinal axis of the long bone, but non-symmetric in the knee structure. The proximal end of the tibia model was enlarged to represent the tibia condyles. The articular surface of the tibia plateau was described with curved surfaces that match with the femur condyle articular surfaces.

The Ligaments - The four ligaments were simulated to connect tibia and femur models. The medial collateral ligament (MCL) and the lateral collateral ligament (LCL) were modeled using four-node Hughes-Liu shell element (Hallquist, 1991) and nonlinear spring element. The 144 shell elements and the 162 spring elements were used for each collateral ligament. The cruciate ligaments (ACL and PCL) were represented by 4 spring damper elements - 2 elements for each cruciate ligament.

The Foot - The foot was represented by 64 eight-node solid hexahedron elements with a concentrated mass 0.9 kg and attached to the distal end of the tibia.

The Upper Body Mass - The upper body was represented by 64 eight-node solid hexahedron elements with a concentrated mass 47 kg attached to the proximal end of the femur.

MATERIAL PROPERTIES - The behavior of living tissues such as long bones, cartilage, and ligaments is non-isotropic, nonlinear/quasi-linear viscoelastic (Viidik, 1987; Cowin, 1989; Fung, 1993). The possibility of modeling such behavior in an explicit FEM code, as for instance DYNA3D, is limited. For this reason, the living tissues in our model were assumed to be isotropic linear viscoelastic material.

The viscoelastic property is described in DYNA3D by the following equation for the shear modulus G :

$$G(t) = G_L + (G_S - G_L)e^{-\beta t}$$

where

G_S = short term shear modulus
 G_L = long term shear modulus
 β = decay constant

Long Bones - Specific material constants were defined for each part of the tibia and femur models to consider the inhomogeneity of the material properties in the tibia and the femur, such as cortical diaphysis, and cancellous epiphyses. The cortical bone forms the wall of the shaft of the long bones, and the cancellous bone was defined at each end.

There is large variation of mechanical properties of living tissues between studies. For instance, Young's modulus of the cortical bone varied from 5 to 25 GPa (Saulgozis et al., 1971; Evans and Vincentelli, 1974; Saulgozis, 1975; Katsamanis and Raftopoulos, 1990), and the range of Young's modulus for the cancellous bone varied from 0.6 to 2.2 GPa (Williams and Lewis, 1982; Ashman et al., 1989; Hvid et al., 1989). In this study, Young's modulus was defined 16.5 GPa for cortical bone, 1.65 GPa for cancellous bone.

Ligaments - The ligaments are composed primarily of collagen and elastic fibers. The behavior of the ligaments is determined by the properties of the collagen and fibers. Considering the structural behavior of the ligaments, the MCL and the LCL ligaments were modeled with nonlinear spring-damper elements in combination with elastic shell elements. The spring elements were placed between nodes of each shell element in the direction of the ligament fiber. In the current study, the simplified geometry of the femur articular surfaces does not enable the implementation of a realistic structural modeling of the cruciate ligaments. Therefore, the ACL and the PCL were modeled with nonlinear spring elements.

The material constants used in the current study are summarized in Table 1. The decay constant β of bone applied in our model was based on the study by Laket and Katz (1979). The decay constant β was estimated with the viscoelastic behavior of human tibia bone in a relaxation period of time 10 s. In the model, the density of bone was adjusted to fit the mass distribution of the lower extremity specimen used in crash tests.

MODELING OF LOWER EXTREMITY SKELETON TO LATERAL IMPACT - The model was implemented by means of the finite element program DYNA3D. In simulations of

dynamic response of the lower extremity skeleton to a lateral impact load, the linear acceleration, the stress distribution was calculated, which yields detailed information related to failure of the knee joint and fracture of the tibia.

Table 1
Material properties of bones and ligaments
(based on Yamada, 1970; Evans, 1973; Cowin, 1989; and Fung, 1993)

Properties	Type of Tissue		
	Compact Bone	Cancellous Bone	Ligaments
E = Young's modulus (MPa)	16500	1650	10
v = Poisson's ratio	0.35	0.35	0.3
ρ = density (kg/m ³)	1850	676	1069
K = Bulk modulus (MPa)	23670	2367	-
G _S (MPa)	7890	789	-
G _L (MPa)	6380	638	-
β	0.5	0.5	-

A stress analysis was performed in terms of the injury mechanism of the lower extremity to a lateral impact loading. Pedestrians involved in car collision accidents usually sustain an impact load from the lateral side. Most tibia fractures are thus attributed to a beam-type bending moments when a car bumper hits the leg from the lateral side. The beam-type bending of the tibia can result in compressive stress in the direct loading side and tensile stress on the opposite side of the tibia. The tibia bending fracture occurs as a results of excessive tensile stress. This phenomenon was simulated using the developed FEM model, and the calculated stress can be used to predict the risk of fracture of long bones under lateral bending load by comparing the calculated stress value with the corresponding ultimate stress in the long bones. In this way, we can also assess the failure of the knee structure such as ligaments and tibia condyles by comparing the calculated parameters with corresponding ultimate strength level.

The strength of the long bones has been investigated in many studies (Yamada, 1970; Saulgozis, 1975; Nyquist, et al., 1985; Katsamanis and Raftopoulos, 1990). The ultimate tensile strength of femoral and tibial cortical bone in bone from 20 to 29 years of age was summarized by Yamada (1970), and it is shown in Table 2. Investigation of age differences in ultimate bending strength of long bones shows that the average strength is the greatest between 20 and 29 years age. In the 50 to 59 age group the strength decreases to about 90% of that in the younger group.

Table 2
Ultimate tensile strength of the cortical bones in the 20 to 29 age group
(Data based on Yamada, 1970)

Bone	σ_t (MPa)
Femur	124
Tibia	143

σ_t = Ultimate tensile strength.

The ultimate strength of the cancellous bone in the long bones, such as femoral and tibial epiphyses, is not available from literature. The ultimate strength of the cancellous bone in the other human body parts can be found from Yamada (1970). For instance, in the lumbar vertebrae the ultimate compressive strength varies from 14 to 19 MPa. These values can be used as a reference to consider the cancellous bone failure in the present study.

VALIDATION OF THE MODEL - The validity of the FEM model was evaluated by comparing the results from simulations and available results from previous tests. The tibia segment of the model was validated against the published three-point bending test with leg specimens (Nyquist, et al., 1985). The whole model was validated against previous tests with lower extremity specimens (Bunketorp, 1983; Aldman, et al., 1985).

Three-Point Bending of the Tibia - A simulation of tibia three-point bending was carried out with the FEM model of the tibia segment. This simulation configuration was based on the

test set-up in an experimental study (Nyquist, et al., 1985). In the study by Nyquist et al. the unembalmed leg specimens were subjected to dynamic three-point bending by a translational impact to the mid-span of the specimens at impact speeds from 2.4 m/s to 4.7 m/s. In these tests, the two reaction forces (Figure 1a) at the two supports were measured. The tensile stress in the mid-span of the tibia was calculated for each specimen based on the reaction force and section modulus of the tibia. Three tests at impact speed 3.7 m/s were chosen to compare with computer simulation of tibia three-point bending. The tensile stresses resulted from these three tests are 150, 138 and 149 MPa (Table 3), and the mean value of the stress from the tests is 146 MPa. At this level of stress, fracture of all tibia specimens were observed.

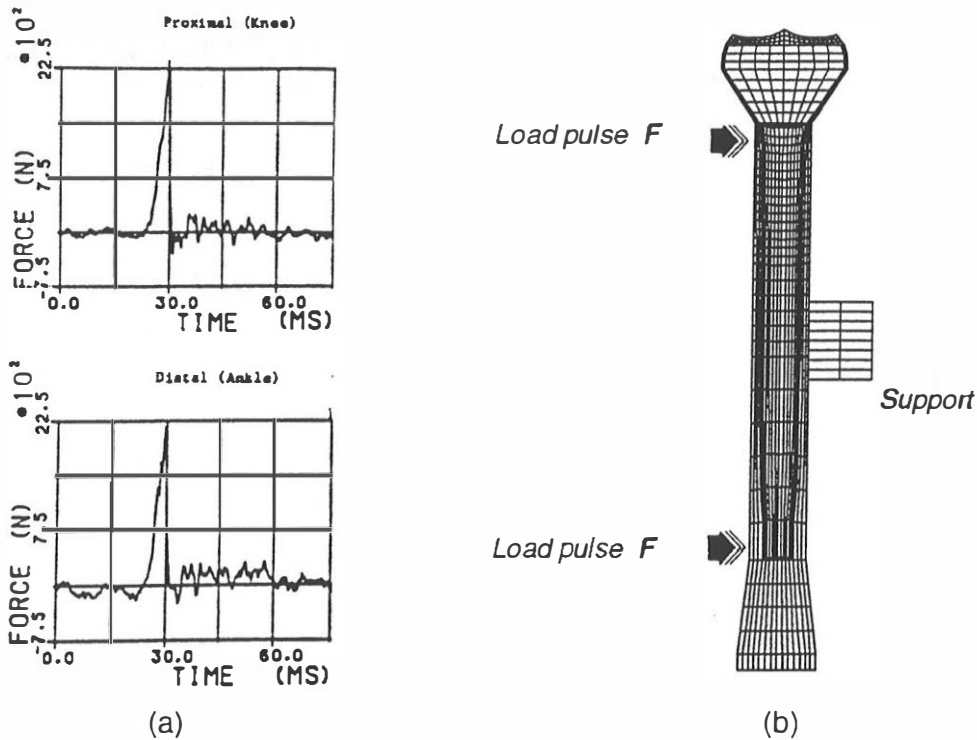


Figure 1. (a) The time history of the reaction force measured in the three-point bending test with leg specimen (adapted from Nyquist et al., 1985); (b) The FEM modeling of three-point bending of the tibia, load pulse F was based on the measured reaction force.

Table 3
Results from the tests of three-point bending of the tibia at 3.7 m/s (based on Nyquist, et al., 1985).

Test No.	Tensile stress (MPa)
127	150
128	138
129	149
Average	146

In the present study, the configuration of FEM modeling the three-point bending of the tibia segment is shown in Figure 1b. The tibia model was supported in the middle span of the tibial shaft by a cylinder which simulated the translational impactor used in the tests. The tibia model was loaded at both proximal and distal ends with forces F (Figure 1) which were measured by Nyquist et al. (1985) in the test at impact speed 3.8 m/s. The distance between the location of the two forces is 260 mm which corresponds to the distance between two supports in the test set-up.

Validation against Test with Lower Extremity Specimen - The FEM model of the lower extremity skeleton system was verified against previous impact tests with lower extremity specimen (Figure 2b) (Bunketorp, 1983; Aldman, et al., 1985). In these tests, the lower extremities were amputated with a part of pelvis. Most of the muscles of the thigh were removed. The specimens were preloaded by a concentrated 47 kg mass connected to the pelvis, and the knees were set at extended position. The whole biomechanical system was then struck by a simulated car-front impactor. The experimental car-front impactor consisted of a bumper and a simulated bonnet structure. For validation of the FEM model, available results from these tests are the bumper impact forces, the linear accelerations of the leg measured near the center of gravity of the leg, and the registered failure of the leg bones and knee ligaments. The results from 10 tests at impact speed 30 km/h and 4 tests at 17 km/h were used in model validation. In the tests at impact speed 30 km/h, tibia fracture was observed in 6 of 10 cases, and the MCL and ACL ruptures occurred in 5 of 10 cases. In the test at impact speed 17 km/h, no long bone fracture occurred, and the ligament rupture was observed in all the cases, especially the MCL rupture occurred in 3 of 4 cases.

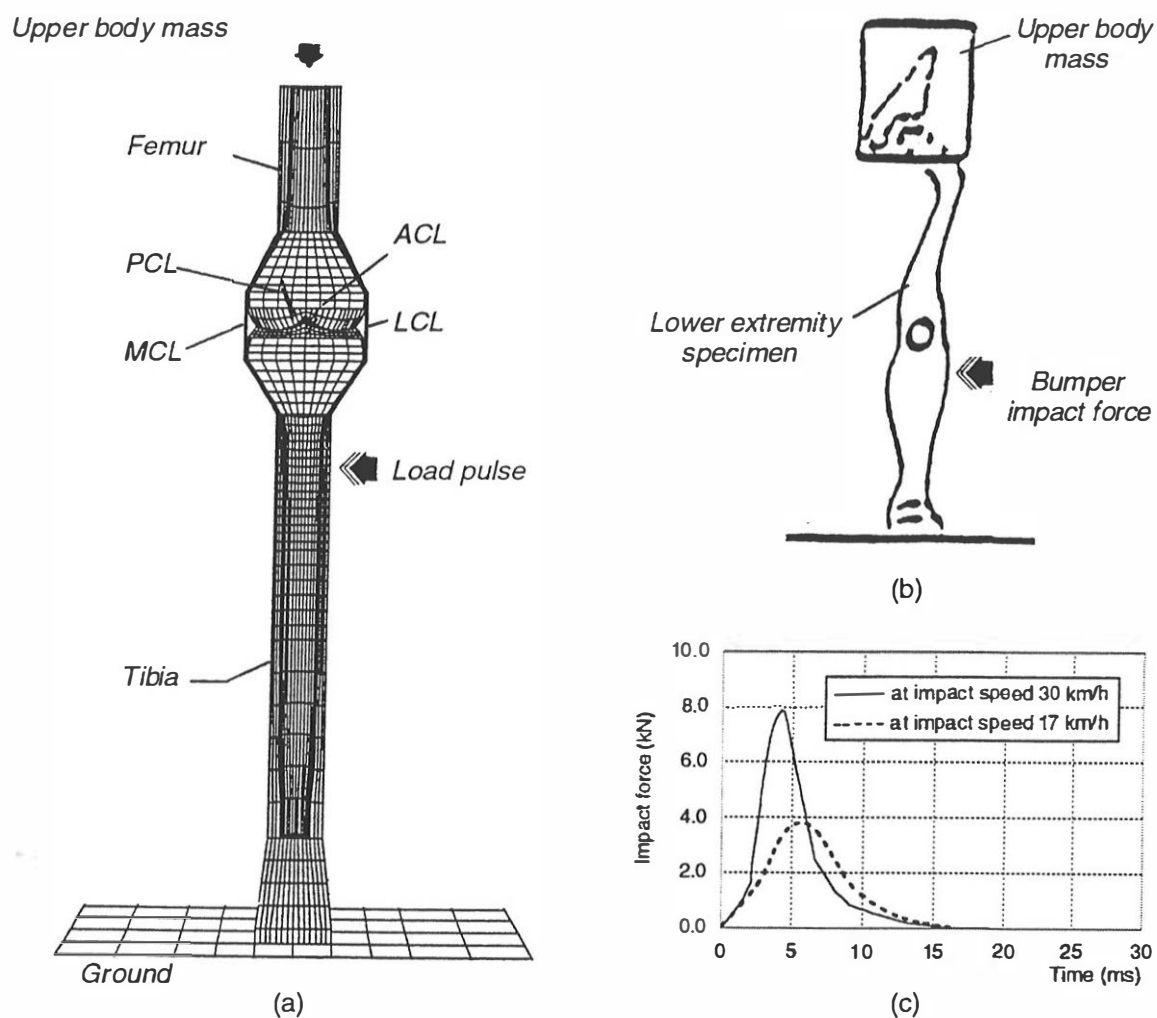


Figure 2. (a) The FEM model of the lower extremity skeleton system subjected to a lateral impact force, ACL-anterior cruciate ligament, PCL-posterior cruciate ligament, MCL-medial collateral ligament, LCL-lateral collateral ligament; (b) The set-up for the impact test with lower extremity specimen; (c) The load pulse used in the model, based on the measured impact forces in the test with lower extremity specimens (Bunketorp, 1983).

Figure 2a shows the FEM model of the lower extremity skeleton system subjected to the lateral impact force below the knee joint. The mass distribution in the model was adjusted

5.5 kg for femur and 3.8 kg for tibia to represent the lower extremity specimens used in crash test (Bunketorp, 1983). The response of the lower extremity skeleton system was simulated in the first 15 ms after impact. During the initial phase of the impact, the force applied to the lower extremity only occurred between protruding bumper and the leg. For this reason, in simulations the lateral bumper impact force to the tibia segment was defined with a load pulse (Figure 2c) from crash tests. Because the load pulse was based on the impact force measured in crash tests with lower extremity specimens, the effect of the bumper impact to the leg bone is equivalent in the model to the impact load pulse. The corresponding peak value of impact force used in simulations was 3.8 kN for 17 km/h and 8 kN for 30 km/h. With this configuration, the response of the FEM model and the results from crash tests with lower extremity specimens are comparable.

RESULTS

The results are presented with peak values of the stress, distribution of the stresses in the mid-coronal plane of the tibia shaft and the knee joint area, the time history plots of stresses, the linear accelerations of the tibia, the ligament elongation, and the relative displacement between articular surfaces.

RESPONSE OF THE TIBIA MODEL - In simulations of the three-point bending of the tibia model, the maximum tensile stress of 157.6 MPa was obtained at element 133 in mid-span of the tibia shaft. Figure 3b illustrates the stress distribution in the mid-coronal plane of the tibia model at 7 ms after impact loading, and the time history of the tensile stress at element 133 is shown in Figure 3a. The results show that the concentrated tensile stress of 157.6 MPa calculated from the simulation corresponds with the stress level 146 MPa from tests by Nyquist et al. (Table 3). A good agreement between results from the simulation and tests was obtained.

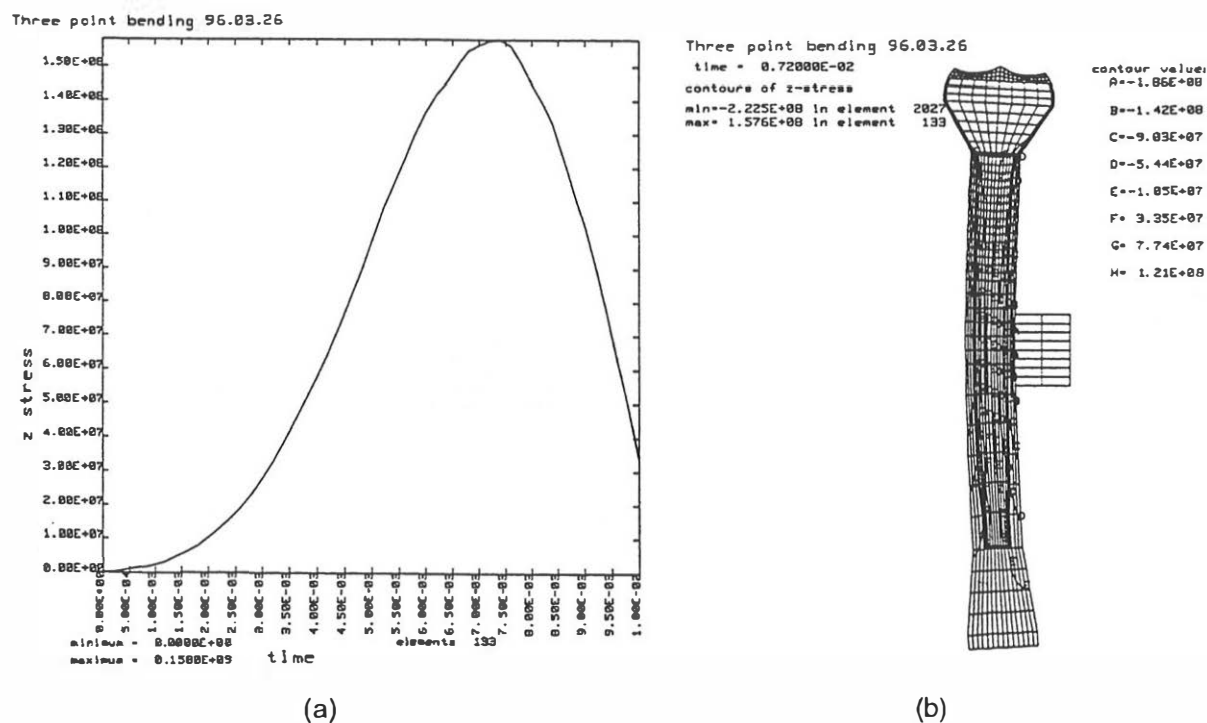


Figure 3. The results from the simulation of three-point bending of the tibia (a) time history of tensile stress; (b) stress distribution within the tibia model.

RESPONSE OF THE LOWER EXTREMITY SKELETON MODEL - Table 4 shows the results from two simulations of the lower extremity skeleton system to lateral impact forces 3.8 kN and 8 kN, including the peak values for the linear accelerations of the tibia, the tensile stresses within the tibia bone, and the elongation of the MCL ligament. Figure 4 illustrates the time history plots of linear accelerations of the leg from simulations and test. Figures 5

and 6 illustrate the stress distribution in the mid-coronal plane of the model for the knee and upper part of the tibia.

Table 4
The peak values from the FEM modeling of the lower extremity skeleton system to a lateral impact

Peak impact force (kN)	3.8	8
Acceleration (g)	140	312
Tensile stress (MPa)	102	160
MCL elongation at 10 ms (mm)	7.5	12
MCL strain at 10 ms (%)	21	34
Transverse dislocation at 8 ms (mm)	9	16

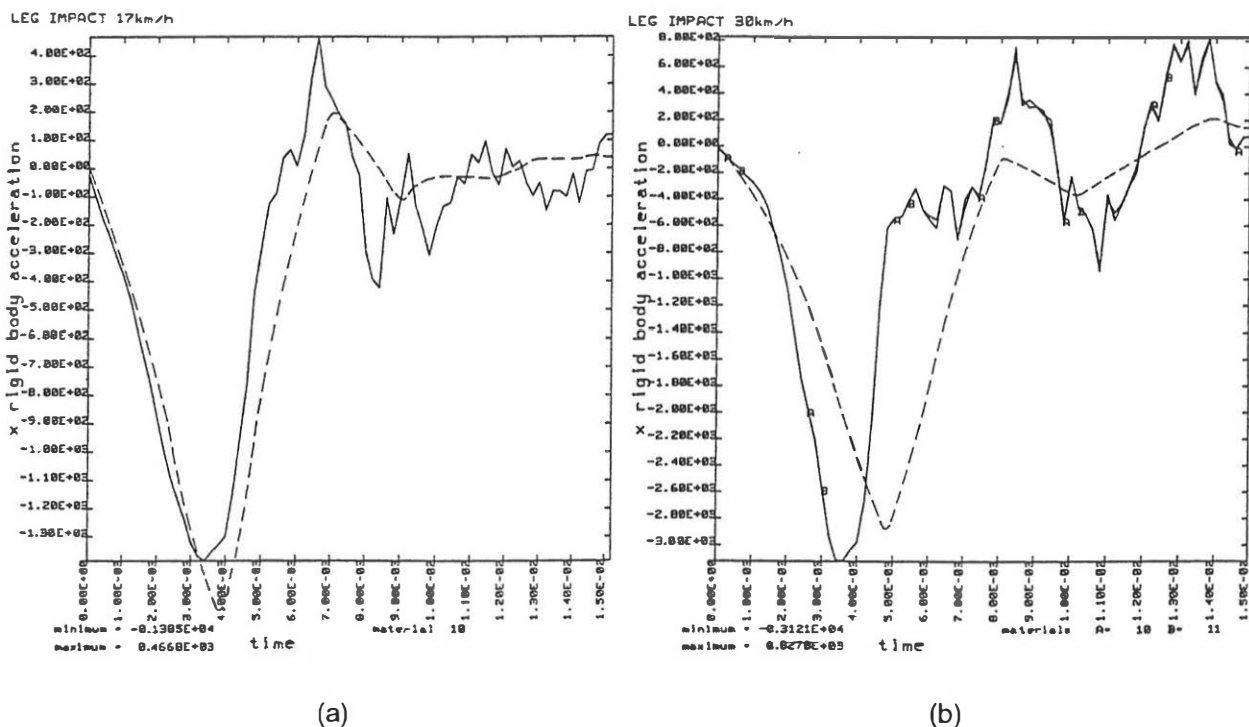


Figure 4. Comparison of the time histories of the linear accelerations of the leg from the simulations (solid line) and tests (dot line) (Bunketorp, 1983): (a) at impact speed 17 km/h; (b) at impact speed 30 km/h.

DISCUSSION

The tibia fracture resulting from lateral bending is one of the important injury mechanism regarding car-pedestrian accidents. Since pedestrians involved in car collisions usually sustain an lateral impact load, most tibia fractures are attributed to bending moments when a car bumper hits the leg from the lateral side. The classical fracture patterns of a beam-type bending failure has been recognized in study by Nyquist et al. (1985). The beam-type bending of the tibia can result in compressive stress in the direct loading side and tensile stress on the opposite side of the tibia (Figure 3). The tibia bending fracture occurs as a results of excessive tensile stress. This phenomenon and the bending strength of the tibia were investigated by using the developed FEM model of the long bones in the present study.

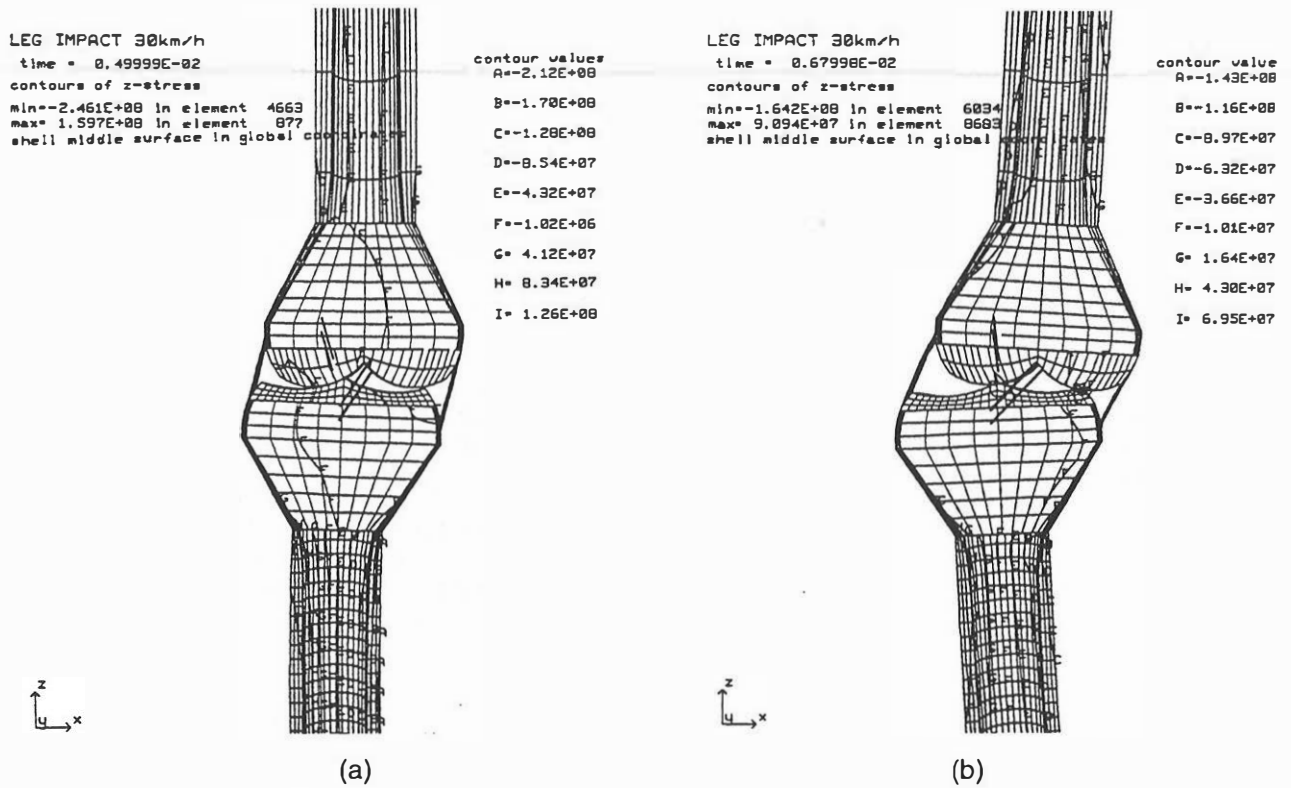


Figure 5. Stress distribution in the knee area from simulation with load pulse at impact speed 30 km/h: (a) at 5 ms, (b) 6.8 ms.

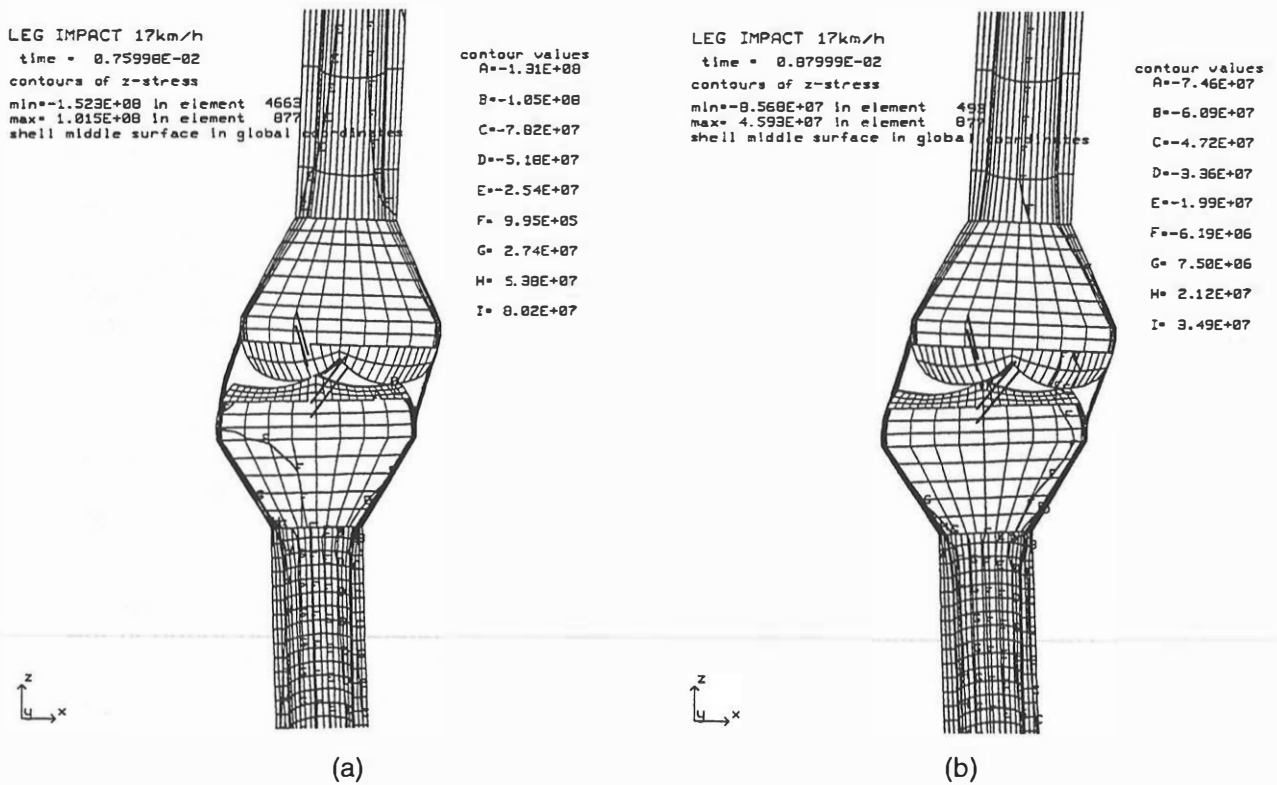


Figure 6. Stress distribution in the knee area from simulation with load pulse at impact speed 17 km/h: (a) at 7.6 ms, and (b) 8.8 ms.

From the simulation of tibia three-point bending we found that the calculated maximum stress has a good agreement with the failure stress resulted from the tests by Nyquist et al. (1985). It indicated that the FEM model is able to predict risk of fracture of the tibia to impact loading.

Based on the test set-up by Bunketorp et al. (1983) we simulated the lower extremity skeleton system to lateral impact force below the knee joint. In this configuration, the similar stress distribution as that in the tibia three-point bending was found in the simulations. This is due to the same mechanism of the bending moment applied to the tibia shaft. The stress concentration due to the tibia lateral bending is observed at the tensile side of the tibia in impact area. At impact speed of 30 km/h, the peak value of the stress increases to 160 MPa 5 ms after impact load. This stress value corresponds to stress level (Table 3) resulting in tibia fracture. The stress response simulates a typical fracture of the tibia called Messerer fracture in car-pedestrian collision accidents. This type of fracture starts on the tensile side of the tibia. At impact speed 17 km/h, the maximum tensile stress is 102 MPa 7.6 ms after impact load. The peak stress occurred later than that for the impact force at 30 km/h. From Figure 6 the stress distribution from the simulation with load pulse at impact speed 17 km/h can be seen. The peak stress level 102 MPa is lower than that for the load pulse at 30 km/h. This level of stress may not result in the long bone failure by comparing the ultimate tensile strength level of the tibia listed in Table 3. In the tests by Bunketorp et al. (1983), the tibia fracture was over-represented at impact speed 30 km/h, but at the impact speed 17 km/h no tibia fracture occurred.

There are another two important modes of response within the knee joint when the leg is subjected to an impact force below the knee: the transverse dislocation between articular surfaces in initial impact phase, and the rotation of the tibia about the knee joint. These two modes of responses correlate with two injury mechanisms: the shearing and bending injuries of the knee joint.

A transverse dislocation between the knee articular interface occurs due to the delay of the femur movement when impact force is transmitted through the knee joint. Analyses of the motion of the knee joint during the transverse response (Figures 5a and 6a) showed that when a lateral impact occurs just below the knee joint the first response of the intra-articular can be transverse motion of the tibia condyle relative to the femur condyle. At the first stage of the impact the proximal end of the tibia was pushed forward in a lateral-medial direction, while the distal end of the femur remains still. At an impact speed of 30 km/h, the first peak transverse displacement of 12 mm was reached about 9 ms after impact, and 13 mm was reached 11 ms after impact at 17 km/h. The shearing displacement leads to the stretching of ligamentous structures of the knee joint and a concentrate contact stress between the medial femur condyle and the tibial intercondylar eminence (Figure 5). The knee resistance to the transverse displacement may primarily result from the contact between the medial femur condyle and the tibial intercondylar eminence. At this moment, there exists increasing contact stresses on the facet of the intercondylar eminence and the medial femoral condyle. The transverse fracture of the tibial intercondylar eminence and/or failure of the femoral cartilage may occur, when the stresses exceed its tolerance level.

A high risk of MCL failure was predicted in this type of impact loading to the knee joint in the simulations. When the knee was laterally bent, the MCL is stretched by a tension force while a compression force is acting on the lateral side of articular interface due to the contact of the lateral condyles. In the simulations, the MCL strain 10 ms after impact was 21% for load pulse at 17 km/h, and 34% for load pulse at 30 km/h. At the same time, concentrate stress might take place at both the medial and the lateral side of the entire knee joint (Figure 5 and 6). The failure of the ligament components could occur in the tension side due to the difference of the ultimate tensile strength of the ligaments and ultimate compressive strength of the bone. The most frequent damage to the knee joint by lateral bending found in the experimental study was avulsion or rupture of the MCL (Bunketorp et al., 1983).

Validation of the FEM model showed that the model enabled the prediction of risk of long bone fracture and knee ligament failure in terms of the stress and strain analysis within the structural model. The model can also be used to analyze the injury mechanism of the knee and fracture of the leg in car-pedestrian collisions. Therefore the model presented in this study can be regarded as a useful tool for investigating the responses of the lower extremity in car-pedestrian collisions.

It is necessary to mention that the ultimate stress level for the long bones can be varied in different age groups in the range of 5 - 15% differences (Yamada, 1970). We did not analyze the influence of the age difference to long bone strength in the present study.

During the past years, there has been increasing interest in FEM modeling of impact responses to human body segments due to the fact that the finite element solution for the human body comes closer to reality in terms of the geometry and material law.

To perfect the current model, extensive validation studies must be carried out, both for a more accurate determination of the material properties and development of model itself, such as soft tissue models, accurate 3-D geometry, various material non-linearity and improved contact model.

CONCLUSIONS

Validation of the FEM model showed that the model makes it possible to predict the risk of long bone fracture and knee joint failure in terms of stress and strain analysis of the lower extremity skeleton system to lateral impact.

The model can also be used to analyze injury mechanisms of the knee under lateral impact loading, such as the shearing and bending injury mechanisms of the knee. The following injury-related parameters can be analyzed: transverse dislocation between tibia and femur articular surfaces, ligament deformation, and stress distribution within the long bones and knee joint structure.

The validated model will therefore be useful for studies of car-pedestrian crash accidents.

REFERENCES

- Kramer, M., Burow, K. and Heger, A. (1973). *Fracture Mechanisms of Lower Legs Under Impact Load*. Proc. of the Seventeenth Stapp Car Crash Conference, Nov 12-13, 1973. Oklahoma City, USA.
- Aldman, B., Kajzer, J., Bunketorp, O. and Eppinger, R. (1985). *An Experimental Study of a Modified Compliant Bumper*. Proc. of the Tenth Int. Technical Conf. on Experimental Safety Vehicles, Oxford England, July 1-4. US Dept of Transportation, NHTSA. 1035-1040.
- Ashman, R.B., Rho, J.Y. and Turner, C.H. (1989): *Anatomical Variation of Orthotropic Elastic Moduli of the Proximal Tibia*. J. Biomechanics, 22, 895-900.
- Bedewi, P.G. and Bedewi, N.E. (1996): *Modelling of Occupant Biomechanics with Emphasis on the Analysis of Lower Extremity Injuries*. IJCrash, Vol. 1 No. 1. 50-72.
- Bermond, F., Ramet, M., Bouquet, R. and Cesari, D. (1993). *A finite element model of the pedestrian knee-joint in lateral impact*. Proc. of the Int. IRCOBI Conf. on the Biomechanics of Trauma, Eindhoven, September 8-10. IRCOBI Secretariat, Bron, France.
- Bunketorp, O. (1983). *Pedestrian Leg Protection in Car Accidents. An Experimental and Clinical Study*. Dept Orthopedic Surgery II, GU and Dept of Traffic Safety, CTH. Ph.D thesis.
- Cowin, S.C. (1989). *Bone Mechanics*. Boca Raton, Florida, CRC Press, Inc.
- Evans, F.G. (1973): *Mechanical Properties of Bone*. Charles C. Thomas Publisher, Illinois, USA.
- Evans, F.G. and Vincentelli, R. (1974): *Relations of the Compressive Properties of Human Cortical Bone to Historical Structure and Calcification*. J. Biomechanics, 7, 1-10.
- Fung, Y.C. (1993). *Biomechanics: Mechanical Properties of Living Tissues*. New York: Springer-Verlag New York, Inc.

- Hallquist, J.O. (1991). *DYNA3D User's Manual: Nonlinear Dynamic Analysis of Structures in Three Dimension*. Livermore Software Technology Corporation, Livermore, USA.
- Hobatho, M.C., Darmana, R., Pastor, P., Barrau, J.J., Laroze, S., and Morucci, J.P. (1991): Development of a Three-Dimensional Finite Element Model of a Human Tibia Using Experimental Modal Analysis. *J. Biomechanics*, Vol. 24, No. 6, 371-383.
- Hvid, I., Bentzen, S.M., Linde, F., Mosekilde, L. and Pongsoipetch, B. (1989): *X-Ray Quantitative Computed Tomography: the Relations to Physical Properties of Proximal Tibial Trabecular Bone Specimens*. *J. Biomechanics*, 22, No. 8/9, 837-844.
- Ishikawa, H., Kajzer, J. and Schroeder, G. (1993). *Computer Simulation of Impact Response of the Human Body in Car-Pedestrian Accidents*. Proc. of the 37th STAPP Car Crash Conference, November 8-10, 1992, San Antonio, Texas, 235-248.
- Kajzer, J. (1991). *Impact Biomechanics of Knee Injuries*. Doctoral Thesis, Department of Injury Prevention, Chalmers University of Technology, Göteborg, Sweden.
- Katsamanis, F. and Raftopoulos, D.D. (1990): *Determination of Mechanical Properties of Human Femoral Cortical Bone by the Hopkinson Bar Stress Technique*. *J. Biomechanics*, Vol.23, No. 11, 1173-1184.
- Nyquist, G. W., Cheng, R., El-Bohy, A. A. R. and King, A. I. (1985). *Tibia Bending: Strength and Response*. Proc. of the 29th STAPP Car Crash Conference, SAE paper 851728, P167, Warrendale, PA, USA.
- Pritz, H. B. (1978). *Comparison of the Dynamic Responses of Anthropomorphic Test Devices and Human Anatomic Specimens in Experimental Pedestrian Impacts*. Proc. of the 22nd Stapp Car Crash Conf, October 24-26, Ann Arbor Michigan, SAE Warrendale Pa., USA. 341-357.
- Saulgozis, Y.Z. (1975): *Difference and Correlation between the Elastic Characteristics of the Compact Bone Tissue of the Human Tibia*. *Polymer. Mech.* 11, 559-663.
- Saulgozis, Y.Z., Knets, I.V., Yanson, A. and Pfafrod, G.O. (1971): *Investigation of the Non Uniform Distribution of the Elastic Strength Characteristics over the Cross Section of the Diaphysis of the Human Tibia*. *Polymer. Mech.* 7, 837-842.
- Viidik, A. (1987): *Properties of Tendons and Ligaments*. Chapter 6, Handbook of Bioengineering, Co-Editors: Skalak, R. and Chien, S. McGraw-Hill Book Company.
- Williams, J.L. and Lewis, J.L. (1982): *Properties of an Anisotropic Model of Cancellous Bone from the Proximal Tibial Epiphysis*. *J. Biomech. Engng.* 104, 50-56.
- Yamada, H. (1970). *Strength of Biological Materials*. Evans, F.G., Ed., Williams & Wilkens, Baltimore.
- Yang, J.K. and Kajzer, J. (1992). *Computer Simulation of Impact Response of the Human Knee Joint in Car-Pedestrian Accidents*. Proc. of the 36th STAPP Car Crash Conference, November 2-4, 1992, Seattle, Washington, USA. 203-218.
- Yang, J.K., Kajzer, J., Cavallero, C., and Bonnoit, J. (1995). *Computer Simulation of Shearing and Bending Response of the Knee Joint to a Lateral Impact*. Proc. of the 39th STAPP Car Crash Conference, November 8-10, 1995, Coronado, California, USA. 251-264.